

COMPUTATION OF BACKWARD-FACING STEP FLOWS BY A SECOND-ORDER REYNOLDS STRESS CLOSURE MODEL

ROBERT R. HWANG AND Y. F. PENG

Institute of Physics, Academia Sinica, Taipei, Taiwan

SUMMARY

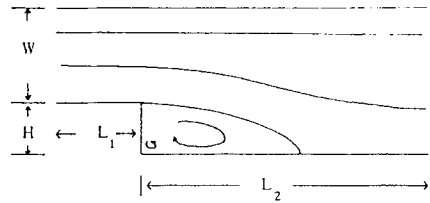
This paper scrutinizes the predictive ability of the differential stress equation model in complex shear flows. Two backward-facing step flows with different expansion ratios are solved by the LRR turbulence model with an anisotropic dissipation model and the near-wall regions of the separated side resolved by a near-wall model. The computer code developed for solving the transport equations is based on the finite-volume–finite-difference method. In the numerical solution of the time-averaged momentum equations the Reynolds stresses are treated partially as a diffusion term and partially as a source term to avoid numerical instability. Computational results are compared with experimental data. It is found that the near-wall region of the separated side resolved by the near-wall model, the LRR model with a simple modification of an anisotropic dissipation model can predict backward step flows well.

KEY WORDS: turbulence model; Reynolds stress model; two-layer approach; backward step flow

1. INTRODUCTION

Flow over a backward-facing step has been extensively studied by many researchers and engineers as the fundamental configuration of internal flow. This flow can be observed in many fluid devices such as gas turbines, jet aircraft engines, wind tunnels, diffusers and turbomachines. The configuration of the flow field is shown in Figure 1. Although the geometry is simple, the flow is complex and the theoretical study of this problem is not easy. Turbulence is itself complicated and the problem becomes more difficult owing to flow separation. Although the Navier–Stokes equations can properly describe turbulent motions in detail, it is too costly and often not necessary for engineers to secure such a complex and detailed solution. Instead, the ensemble-averaged Navier–Stokes equations and turbulence model are often considered to be sufficient and practical to describe turbulent motions.

In the second-order closure of the turbulence model the standard k – ε model has been successfully applied to a large number of flows such as simple shear flows,¹ a buoyant jet in a cross-flow² and complex wall shear flows with a one-equation turbulence model near the wall.^{3–5} The eddy viscosity model, however, makes a basic assumption that the Reynolds stress is aligned with the velocity gradient. This assumption is correct in simple shear flows but is not valid for complex flows such as 3D flows⁶ and asymmetric channel flows.⁷ Hence, in order to avoid any unreasonable prediction results, a differential Reynolds stress equation model is necessary for predicting complex flows. Among the Reynolds stress closure turbulence models which can predict more precisely a turbulent flow field at the expense of solving the differential equations for every Reynolds stress component, the LRR turbulence model⁸ has been tested in some simple free as well as wall shear flows and satisfactory



$$\text{STEP1: } R_H = \nu U_0 / H = 3.7 \times 10^4, \quad W = 8H, \quad L_1 = 4H, \quad L_2 = 30H$$

$$\text{STEP1: } R_H = \nu U_0 / H = 5.4 \times 10^4, \quad W = 2H, \quad L_1 = 4H, \quad L_2 = 16H$$

Figure 1. Nomenclature and geometric boundaries of step flow

results have been obtained. Lakshminarayana⁶ pointed out that the Reynolds stress model has more potential than the $k-\varepsilon$ model when applied to the prediction of complex shear flows.

The overall success of all modern turbulence models in internal as well as external flows is determined in large measure by the treatment of boundary conditions at solid walls. In applications of turbulence models the most popular near-wall treatment is the wall function method. Unfortunately, calculations of backward step flows with wall functions lead to more than 20% error in the reattachment length.^{5,9} This is because although the basic assumptions made in the wall function approach, i.e. flow parallel to the wall and equilibrium turbulence relations, are correct for simple wall shear flows, a certain error will be created when the method is applied to complex wall shear flows.

An alternative to the use of wall functions is to employ turbulence models which are valid all the way to the wall. In recent years many researchers have tried to develop low-Reynolds-number models by incorporating either a wall damping effect or a direct effect of molecular viscosity, or both, in the empirical constants and functions in the turbulence transport equations derived originally for high-Reynolds-number, fully turbulence flows far from the wall. Several low-Reynolds-number models have been reviewed by Patel *et al.*¹⁰ and Michelassi and Shih.¹¹ In separated flows, however, low-Reynolds-number models have been little tested so far. Previous calculations indicated that the damping functions developed for attached boundary layers are not always well behaved in separated flows.⁴

In order to save grid points and hence computer storage and time, to increase the robustness of the method and also to introduce the fairly well-established length scale distribution very near the walls into the turbulence model, the use of a two-layer model becomes more effective. In two-layer models the near-wall viscosity-affected regions are resolved, where the dissipation rate of the turbulent kinetic energy ε is determined by a prescribed length scale distribution l_ε instead of by the transport differential equation. A variety of two-dimensional boundary layer and separated flows have been tested with two-layer models, e.g. adverse pressure gradient boundary layer flows³ and flows with secondary reverse flow.⁴ It has been found that two-layer models can predict more promising results than those of low-Reynolds-number models or the wall function approach. Hence it is concluded¹⁴ that two-layer models are promising tools for practical applications in flows where wall functions are either not applicable or inaccurate and where low-Reynolds-number models are not well behaved or too costly.

Most two-layer models currently used adopt the two-equation $k-\varepsilon$ turbulence model in the calculation of the flow field remotely from the wall; the turbulent transport equation solved in the near-wall layer is the k -equation only, which is formally identical with the popular one-equation model of the 1970s. It is rare for the Reynolds stress equation model to be employed in the field of two-layer modelling. This may be due to the fact that the Reynolds stresses in the mean flow momentum equations are treated as a source term, which will lead to some additional numerical difficulty in the numerical computation. The appearance of a large source term in turbulent flow creates stiffness and

numerical instability. This difficulty has discouraged many researchers from venturing to use the Reynolds stress model.

In the present study a flat plate boundary layer and two two-dimensional backward-facing step flows, denoted STEP1 and STEP2, are solved by the LRR turbulence model with an anisotropic dissipation model in the framework of the two-layer modelling concept. The flat plate boundary layer is chosen as a test case. The STEP1 flow is an experimental study of flow¹² which was designed to test the predictive ability of turbulence models and the STEP2 is benchmark flow problem number 0421 of the Stanford Conference in 1981,⁹ with expansion ratios of 1.125 and 1.5 respectively. The geometric boundaries of the STEP1 and STEP2 flows are indicated in Figure 1. The purpose of this study is to verify the predictive ability of the Reynolds stress closure turbulence model in applications of complex wall shear flows by using the two-layer modelling concept and also to establish a calculation method which can avoid the numerical instability created by the large source term of the momentum equations when using the differential stress equation model. In the numerical iterations of this study the Reynolds stresses in the mean flow momentum equation are treated partially as a diffusion term and partially as a source term. It is seen from the iteration history that this treatment of the Reynolds stresses leads to a good conversion of the momentum equations. In the comparison of computational results with experimental data it is found that the LRR turbulence model with an anisotropic dissipation model can show good performance in predicting backward step flows.

2. GOVERNING EQUATIONS AND SIMULATION CONCEPTS

The exact Reynolds-averaged equations of continuity and momentum for two-dimensional, unsteady, incompressible fluid flow are

$$\frac{\partial U}{\partial X} + \frac{\partial V}{\partial Y} = 0, \quad (1)$$

$$\frac{\partial U}{\partial t} + U \frac{\partial U}{\partial X} + V \frac{\partial U}{\partial Y} = \frac{\partial}{\partial X} \left(\nu \frac{\partial U}{\partial X} \right) + \frac{\partial}{\partial Y} \left(\nu \frac{\partial U}{\partial Y} \right) - \frac{\partial}{\partial X} (\overline{uu}) - \frac{\partial}{\partial Y} (\overline{uv}) - \frac{1}{\rho} \frac{\partial P}{\partial X}, \quad (2)$$

$$\frac{\partial V}{\partial t} + U \frac{\partial V}{\partial X} + V \frac{\partial V}{\partial Y} = \frac{\partial}{\partial X} \left(\nu \frac{\partial V}{\partial X} \right) + \frac{\partial}{\partial Y} \left(\nu \frac{\partial V}{\partial Y} \right) - \frac{\partial}{\partial X} (\overline{uv}) - \frac{\partial}{\partial Y} (\overline{vv}) - \frac{1}{\rho} \frac{\partial P}{\partial Y}, \quad (3)$$

where (U, V) and (u, v) are the mean velocity components and fluctuating velocity components in directions (X, Y) respectively, t is time, P is the mean pressure, ν is the molecular kinematic viscosity and $(\overline{uu}, \overline{uv}, \overline{vv})$ are the Reynolds stresses. These equations can be solved for (U, V, P) when a suitable turbulence model is employed for the Reynolds stress distributions. In this study the LRR turbulence model with an anisotropic dissipation model is used for this purpose, i.e.

$$\begin{aligned} \frac{D\overline{u_i u_j}}{Dt} = C_s \frac{\partial}{\partial X_k} \left[\frac{k}{\varepsilon} \left(\overline{u_i u_l} \frac{\partial \overline{u_j u_k}}{\partial X_l} + \overline{u_j u_l} \frac{\partial \overline{u_i u_k}}{\partial X_l} + \overline{u_k u_l} \frac{\partial \overline{u_i u_j}}{\partial X_l} \right) \right] \\ + \mathbb{P}_{ij} - \frac{\varepsilon \overline{u_i u_j}}{k} - C_1 \frac{\varepsilon}{k} (\overline{u_i u_j} - \frac{2}{3} \delta_{ij} k) - C_2 (\mathbb{P}_{ij} - \frac{2}{3} \delta_{ij} \mathbb{P}), \end{aligned} \quad (4)$$

$$\frac{Dk}{Dt} = \frac{\partial}{\partial X_l} \left(C_k \frac{k^2}{\varepsilon} \frac{\partial k}{\partial X_l} + \nu \frac{\partial k}{\partial X_l} \right) + \mathbb{P} - \varepsilon, \quad (5)$$

$$\frac{D\varepsilon}{Dt} = C_\varepsilon \frac{\partial}{\partial X_k} \left(\frac{k}{\varepsilon} \overline{u_k u_l} \frac{\partial \varepsilon}{\partial X_l} \right) + C_{\varepsilon 1} \frac{\varepsilon}{k} \mathbb{P} - C_{\varepsilon 2} \frac{\varepsilon^2}{k}, \quad (6)$$

where

$$\mathbb{P}_{ij} = -\left(\overline{u_i u_j} \frac{\partial U_j}{\partial X_i} + \overline{u_j u_i} \frac{\partial U_i}{\partial X_j}\right), \quad \mathbb{P} = -\overline{u_i u_i} \frac{\partial U_i}{\partial X_i}.$$

The dissipation model in the above Reynolds stress equations represented by the underlined term was proposed by Rotta¹³ (1951) and is normally used to correct the near-wall anisotropic behaviour of the dissipation rate of the Reynolds stresses. The moduli used in the LRR turbulence model are adopted in this study as $C_s = 0.11$, $C_1 = 1.5$, $C_2 = 0.6$, $C_\varepsilon = 0.15$, $C_{\varepsilon 1} = 1.44$ and $C_{\varepsilon 2} = 1.90$.

In the viscosity-affected regions near the wall of the separated side these turbulent equations were modified analytically to the near-wall approach method of Chen and Patel.³ Specifically, the turbulent diffusion terms of the LRR turbulence model, i.e. $C_s(\partial/\partial X_k)[(k/\varepsilon)(\overline{u_i u_l} \partial \overline{u_j u_k} / \partial X_l + \overline{u_j u_l} \partial \overline{u_k u_i} / \partial X_l + \overline{u_k u_l} \partial \overline{u_i u_j} / \partial X_l)]$, were written as $(\partial/\partial X_k)(\nu_t \partial \overline{u_i u_j} / \partial X_k)$, where ν_t is given by

$$\nu_t = C_\mu k^{1/2} l_\mu \quad (7)$$

and ε is determined from

$$\varepsilon = k^{3/2} / l_\varepsilon. \quad (8)$$

The length scales l_μ and l_ε are adopted from the model

$$l_\mu = C_l Y [1 - \exp(-R_Y / A_\mu)], \quad (9)$$

$$l_\varepsilon = C_l Y [1 - \exp(-R_Y / A_\varepsilon)], \quad (10)$$

where both length scales contain damping effects in the near-wall region in terms of the turbulence Reynolds number $R_Y = k^{1/2} Y / \nu$. Here Y is the normal distance from the wall. The turbulence model moduli are given as $C_l = \kappa C_\mu^{3/4}$, $A_\varepsilon = 2C_l$ and $A_\mu = 70$, where κ is the Karman constant and $C_\mu = 0.09$.

In conducting the computation, the two models have to be matched at some location in a region where viscous effects have become negligible. In this study, preselected grid lines are set for matching the two models within the criterion $R_y \geq 250$ recommended by Chen and Patel.³

3. BOUNDARY CONDITIONS

Four boundary conditions for each of the governing equations (1)–(6) are required to make the problem well posed. The inlet boundary conditions were specified at a location four times the step height (H_1 or H_2) upstream of the steps. For the velocity profiles there U was specified from the one-seventh power distribution to recover the measured boundary layer thicknesses $\delta_1/H_1 = 0.24$ and $\delta_2/H_2 = 1.5$ for STEP1 and STEP2 respectively and $V = 0$. The turbulent transport quantities were specified by the following values appropriate to fully developed turbulent flow assigned there:

$$k = 0.04U^2, \quad \varepsilon = 0.09k^{3/2}/H, \quad -\overline{uv} = 0.25k, \quad \overline{uu} = 0.67k, \quad \overline{vv} = 0.67k.$$

The outlet boundary conditions were specified at locations $30H_1$ and $16H_2$ downstream of the steps for STEP1 and STEP2 respectively. From the experimental data it is found that the mean velocities and turbulent quantities are all approximately fully developed. The normal gradients of all quantities were taken to be zero.

At the fixed walls the boundary conditions were specified as $U = V = \overline{uv} = \overline{uu} = \overline{vv} = k = \varepsilon = 0$.

4. NUMERICAL TECHNIQUE

In this study the computations were performed on a non-uniform and staggered MAC (marker-and-cell) grid system. In the staggered grid system the pressure and the other dependent turbulent variables $\bar{u}\bar{v}$, $\bar{u}\bar{u}$, $\bar{v}\bar{v}$, k and ε are calculated at nodal points between those for the mean velocity. In the computations the grid numbers are 100×82 for STEP1 and 100×64 for STEP2 and 10 grids are set across the near-wall layer in the computations of the near-wall boundary.

To solve the partial differential equations (2)–(6), a computer code based on the power law difference (PLD) method was constructed for use in the present study. Briefly, the convection and diffusion terms of the transport equation for ϕ ($\phi = U, V, k, \varepsilon, \bar{u}\bar{u}, \bar{v}\bar{v}, \bar{u}\bar{v}$), i.e.

$$\partial(U_j\phi)/\partial X_j = \partial(\Gamma\partial\phi/\partial X_j)/\partial X_j + S_\phi,$$

are discretized by the power law difference and the source term by the second-order central difference and these are then integrated within a control volume element to obtain an algebraic equation. The pressure field P is solved with the SIMPLEC algorithm of Von-Doornaal and Raithby.¹⁴ The system of linear algebraic equations is solved by the alternating direction line-by-line iteration method.

It should be pointed out that when applying the PLD method to solve the mean flow momentum equation with the differential Reynolds stress equations, some special arrangement is required to treat the source terms. It is known that the PLD method is an approximation to the exponential difference (ED) method¹⁵ which was originally developed and extended from the exact solution of the one-dimensional transport equation in which only convection and diffusion terms are present. From this point of view the PLD method offers a fine differencing method analogous to the analytic differencing methods for convection and diffusion terms. In addition, source terms are often the cause of divergence in the iteration of the transport equations, especially for the momentum equations of mean flow in which the source terms are large.

It is known that the turbulent shear stress is often several orders larger than the molecular shear stress in turbulent flows. The appearance of large source terms in equation (2) creates a stiffness derivative and hence causes numerical instability in the numerical iterations. In simple shear flow calculations the turbulent shear stress $-\bar{u}\bar{v}$ in the momentum equation is usually divided and multiplied by the velocity gradient $\partial U/\partial Y$, i.e. $\partial(-\bar{u}\bar{v})/\partial Y = \partial\{[-\bar{u}\bar{v}/(\partial U/\partial Y)] \times (\partial U/\partial Y)\}/\partial Y$, and $-\bar{u}\bar{v}/(\partial U/\partial Y)$ is treated as an eddy viscosity. In doing this, the turbulent shear stress is effectively cast into the diffusion term. However, in elliptic-type flows the velocity gradients will not always have the same sign as the turbulent shear stresses as they do in simple shear flows. When the velocity gradient and the turbulent shear stress are of opposite sign, negative nodal coefficients will be introduced. The presence of a negative nodal coefficient can lead to numerical instability, since the negative nodal coefficient will create a negative diffusion and consequently a physically unrealistic solution such that the solution will not converge. The appearance of numerical instability in calculating the turbulent Navier–Stokes equations with the differential stress equations was also reported by Amano and Goel,¹⁶ Huang and Leschziner¹⁷ and Brankovic and Syne¹⁸.

The technique used in this study to overcome the numerical instability of the momentum equations is a modification of the numerical procedure of the eddy viscosity model. With the addition and subtraction of the eddy viscosity approximations $-\bar{u}\bar{u}_j = (C_\mu k^2/\varepsilon)(\partial U_i/\partial X_j + \partial U_j/\partial X_i) - \frac{2}{3}\delta_{ij}k$ and $C_\mu = 0.09$ the Reynolds stresses can be expressed as

$$\begin{aligned} -\bar{u}\bar{u} &= -\bar{u}\bar{u} + C_\mu \frac{k^2}{\varepsilon} \left(\frac{\partial U}{\partial X} + \frac{\partial U}{\partial X} \right) - \frac{2}{3}k - C_\mu \frac{k^2}{\varepsilon} \left(\frac{\partial U}{\partial X} + \frac{\partial U}{\partial X} \right) + \frac{2}{3}k, \\ -\bar{u}\bar{v} &= -\bar{u}\bar{v} + C_\mu \frac{k^2}{\varepsilon} \left(\frac{\partial U}{\partial Y} + \frac{\partial V}{\partial X} \right) - C_\mu \frac{k^2}{\varepsilon} \left(\frac{\partial U}{\partial Y} + \frac{\partial V}{\partial X} \right). \end{aligned}$$

Substituting the above expressions into the momentum equation (2), the following equation is obtained:

$$\begin{aligned} \frac{\partial U}{\partial t} + U \frac{\partial U}{\partial X} + V \frac{\partial U}{\partial Y} = & \frac{\partial}{\partial X} \left[\left(\nu + C_\mu \frac{k^2}{\varepsilon} \right) \frac{\partial U}{\partial X} \right] + \frac{\partial}{\partial Y} \left[\left(\nu + C_\mu \frac{k^2}{\varepsilon} \right) \frac{\partial U}{\partial Y} \right] \\ & - \frac{\partial}{\partial X} (\overline{uu}) - \frac{\partial}{\partial X} \left[\left(C_\mu \frac{k^2}{\varepsilon} \right) \frac{\partial U}{\partial X} \right] \\ & - \frac{\partial}{\partial Y} (\overline{uv}) - \frac{\partial}{\partial Y} \left[\left(C_\mu \frac{k^2}{\varepsilon} \right) \frac{\partial U}{\partial Y} \right] - \frac{1}{\rho} \frac{\partial P}{\partial X}. \end{aligned} \quad (11)$$

Physically, equation (11) is formally identical with equation (2) and no additional error is created. Numerically, however, the main Reynolds stresses are cast into turbulent diffusion forms $(\partial/\partial X)[(C_\mu k^2/\varepsilon)\partial U/\partial X]$ and $(\partial/\partial Y)[(C_\mu k^2/\varepsilon)\partial U/\partial Y]$, which can be applied via the PLD method in the numerical solution, and the rest into source terms $-\partial\overline{uu}/\partial X - \partial[(C_\mu k^2/\varepsilon)\partial U/\partial X]/\partial X$ and $-\partial\overline{uv}/\partial Y - \partial[(C_\mu k^2/\varepsilon)\partial U/\partial Y]/\partial Y$, which are trivial and have no serious effect on the numerical stability of the momentum equation; the central difference method is then applied. The accuracy and convergence of the numerical method have been tested by solving a boundary layer flow with zero pressure gradient and two step flows in this study.

5. RESULTS AND DISCUSSION

5.1. Test case

The test case considered is a high-Reynolds-number, flat plate boundary layer flow. The computation is performed on a 40×50 grid system non-uniformly distributed in a $W \times 30W$ fluid domain attached to a fixed flat plate. The inlet condition is a uniform flow with velocity U_0 and turbulent intensity 0.2%. The computational results of the present Reynolds stress closure model through the two-layer modelling concept are shown in Figure 2. The figure presents the mean velocity and turbulent shear stress distributions across the boundary layer at the location X where the Reynolds number $U_0 X/\nu$ equals 3.6×10^6 . A comparison of numerical results with experimental data¹⁹ indicates that the Reynolds stress closure turbulence model predicts the mean velocity and turbulent shear stress profiles in good agreement with the experimental data. Even in the near-wall region the agreement is almost perfect. This illustrates that the near-wall turbulence model of the two-equation turbulence model is well behaved when combined with the differential Reynolds stress equation model in solving turbulent shear flows.

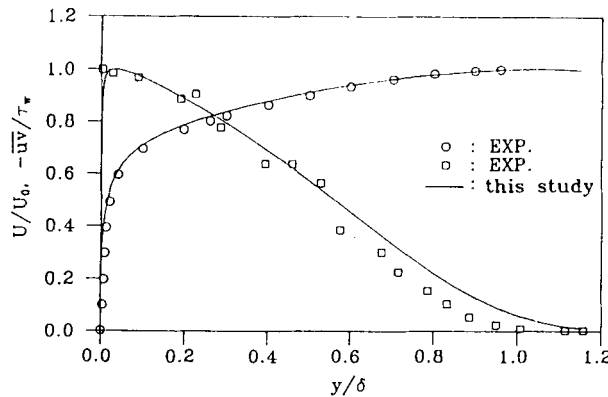


Figure 2. Mean velocity and Reynolds shear stress distributions of flat plate boundary layer flow

The computation of the flat plate boundary layer flow provides a good test case for the numerical method. From the iteration history plot in Figure 3 it is seen that the above treatment of the Reynolds stresses in the momentum equation leads to good convergence. We also tested the computation without the treatment of the Reynolds stresses and found that the computational effort required then is much greater. Because of the limitations of our computing resources, the computation without the treatment of the Reynolds stresses has not been thoroughly completed even in this simple test case. It should be remarked here that the adoption of a differential Reynolds stress model leads to the difficulty that the Reynolds stresses in the momentum equation are treated as a source term in the numerical solution of the mean flows, and the appearance of large source terms in turbulent flows creates stiffness and hence numerical instability. The large source terms of the turbulence Reynolds stresses also mean that the higher accuracy of convection term schemes such as QUICK does not apply to turbulent flows easily. In the present study we provide a simple way to overcome this numerical difficulty by using the PLD scheme.

5.2. Backward-facing step flows

Figure 4 shows the calculated streamline contours of STEP1. It is seen that the flow pattern of the step flow separates at the step corner, recirculates behind the step and then reattaches downstream. Near the lower step corner there is a small secondary recirculation zone. The horizontal distance from the step corner ($X=0$) to the reattachment point ($X=X_R$) is called the reattachment length.

To verify the predictive ability of turbulence models, the first consideration is the prediction of gross parameters of the flow fields, among which the reattachment length is a sensitive parameter that has historically been used to assess the overall predictive ability of turbulence models. Table I lists the predicted reattachment lengths of backward step flows of the $k-\varepsilon$ and present models and compares them with the measured data. It is found that the reattachment lengths obtained using the 'two-layer model' are in better agreement with the measurements than those obtained using the 'wall function'. It is also found that the predicted reattachment length of this study fitted the measured data fairly well and was better than that of the $k-\varepsilon$ model. This can be taken as a first indication that the Reynolds stress closure model is valid for predicting complex shear flows.

Figures 5 and 6 show the distributions of the step-side wall static pressure along the flow obtained by the Reynolds stress closure model for STEP1 and STEP2 respectively. In both cases the agreement

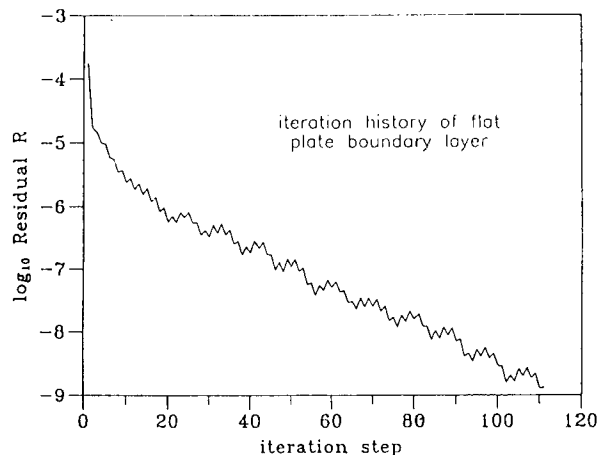


Figure 3. Iteration history of flat plate boundary layer flow

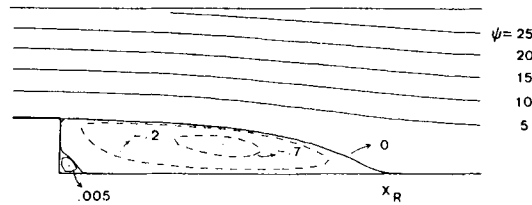


Figure 4. Predicted streamlines of STEP1 flow in region of $(-H: 8H, 0: 3H)$

with the measured data is seen to be quite good. The streamwise mean velocity profiles of STEP1 and STEP2 at various sections are plotted in Figures 7 and 8 respectively. In the STEP1 case the calculated results of the $k-\epsilon$ model⁵ are also shown for comparison. In both cases the computational results of this study exhibit good agreement with the measured data. As seen in Figure 6, the computational results of the $k-\epsilon$ model generally fit the measured data well except in the reverse flow region. Where the $k-\epsilon$ model overpredicts the velocity gradient near the step-side wall, it also overpredicts the wall friction coefficient C_f . This is illustrated in Figure 9, which shows the distributions of C_f along the step-side wall of STEP1. Because of the absence of a measure profile of C_f for the STEP2 flow, the calculated C_f -values of STEP2 are plotted in Figure 10 in natural co-ordinates, i.e. all distances in the streamwise direction are normalized by the reattachment length $-X^* = (x_R - x)/x_R$, and compared with various experimental data.²⁰ It is known that data from various backward step experiments tend to collapse when plotted using X^* -co-ordinates. From Figures 9 and 10 it is seen that the computational results of this study fit the experimental data well. It is also found that there is a positive value of C_f obtained at a short distance from the lower step corner ($X = 0$), which indicates that a small secondary eddy existed around the lower step corner. The secondary eddy has also been observed in the experiments of Driver and Seegmiller.¹²

To illustrate the suitability of the near-wall approach method clearly, Figure 11 shows the near-wall model calculations and the measured velocity distributions in the reverse flow region in wall co-ordinates; the standard logarithmic distribution is also plotted for comparison. It is clear that the measured profile deviates significantly from the logarithmic distribution, while the calculations of the present study fit the measured data well. It is known that the wall function method is not appropriate for some specific flows, e.g. separated flows, flows non-parallel to the wall and three-dimensional flows, nor in the reverse flow region behind a step. Since the wall function approach was derived based on the assumptions that the flow is parallel to the wall and the turbulent field is under equilibrium, errors will certainly be introduced by applying this method to flows which do not meet those requirements. On the other hand, the near-wall model adopted in this study appears to be promising near-wall approach method when applied to complex wall shear flows. It is also evidence that the near-wall flow treatment of this study is suitable.

Table I. Separation lengths of STEP1 and STEP2

		Separation length X_R/H		
		$k-\epsilon$	This study	Exp
STEP1	Wall function	4.2	NA	6.2
	Two-layer model	5.2	6.1	
STEP2	Wall function	5.2-5.9	NA	7 ± 1
	Two-layer model	NA	7.0	

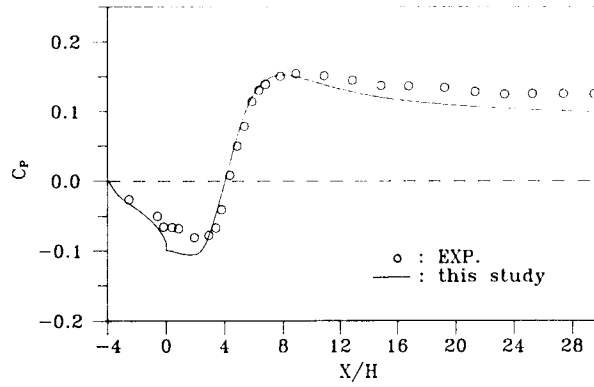


Figure 5. C_p along bottom wall of STEP1

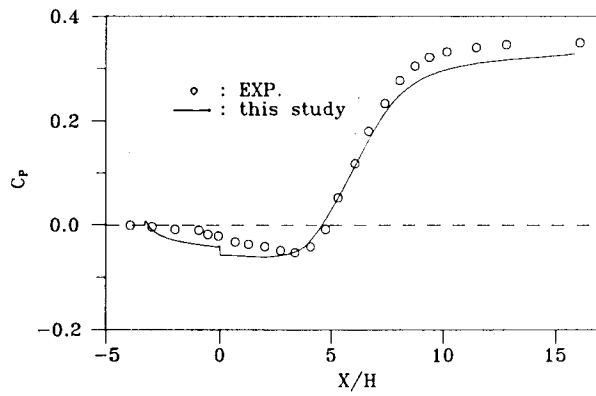


Figure 6. C_p along the bottom wall of STEP2

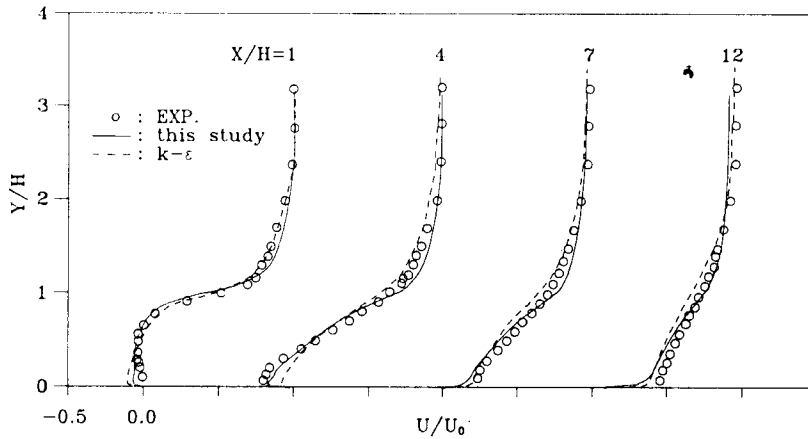


Figure 7. Mean velocity distribution of STEP1

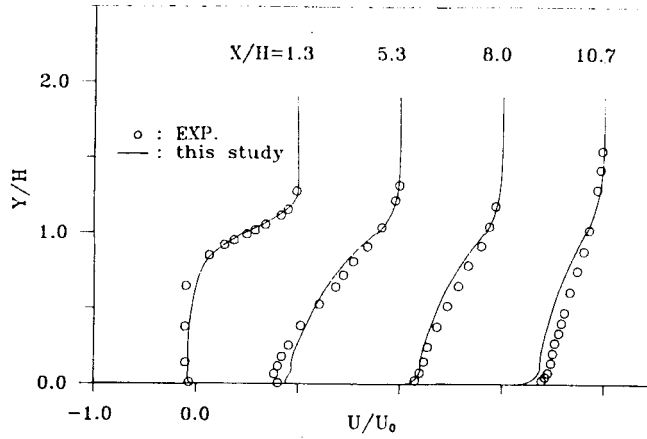


Figure 8. Mean velocity distribution of STEP2

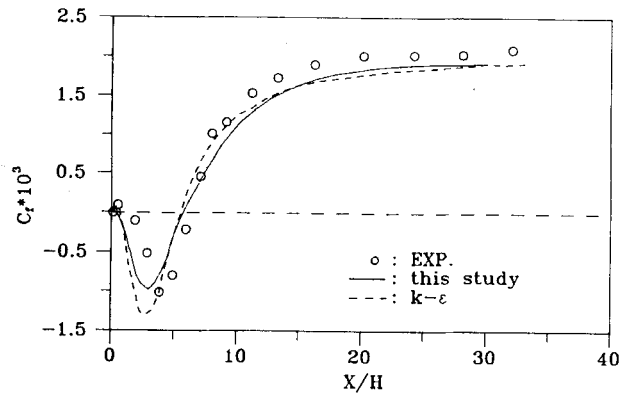


Figure 9. C_f along bottom wall of STEP1

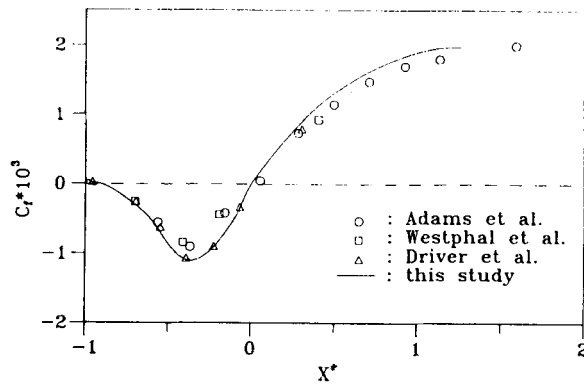


Figure 10. C_f along bottom wall of STEP2

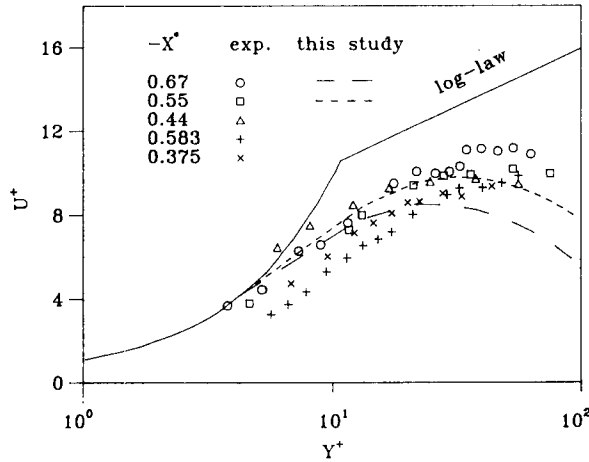


Figure 11. Reverse flow distributions of step flow in wall co-ordinates

Figures 12 and 13 show the profiles of the Reynolds shear stress across the flow at various sections for STEP1 and STEP2 respectively. From these figures it is also seen that the Reynolds stress closure turbulence model with the near-wall two-layer approach exhibits good agreement with experimental data.

6. CONCLUDING REMARKS

In the present study the LRR turbulence model with a simple modification of Rotta's dissipation model is applied to predict backward-facing step flows within the two-layer modelling concept. From the comparison with experimental data it is found that the present model gives a better prediction of the reattachment length in both STEP1 and STEP2 flows than that of other turbulence models. It is also found that the predicted C_p , C_f , velocity and turbulent stress distributions are very realistic, thus confirming that with a simple modification of the dissipation model the LRR turbulence model can predict backward step flows well.

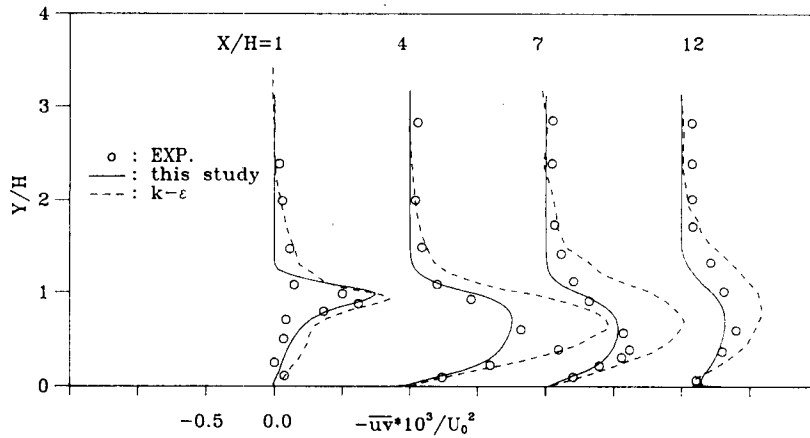


Figure 12. Reynolds shear stress distribution of STEP1

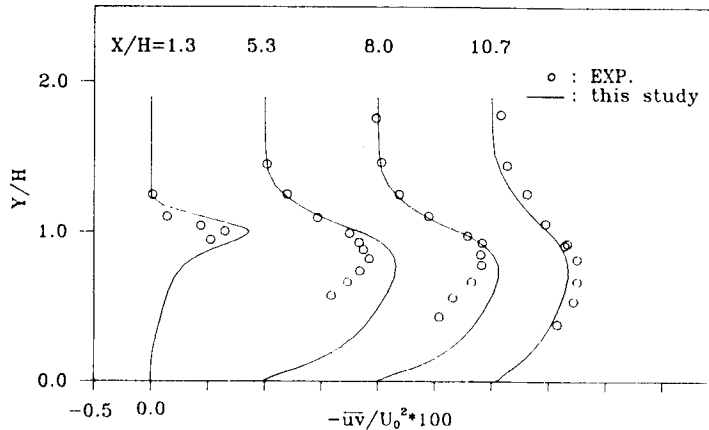


Figure 13. Reynolds shear stress distribution of STEP2

In the numerical solution of the time-averaged momentum equations the Reynolds stresses are treated partially as a diffusion term and partially as a source term. From the iteration history it is found that this simple treatment leads to a good conversion in solving the time-averaged momentum equations numerically.

ACKNOWLEDGEMENT

The work reported herein was performed under National Science Council of the Republic of China grant NSC82-0209-E001-012. This support is gratefully acknowledged.

REFERENCES

1. B. E. Launder, A. Morse, W. Rodi and D. B. Spalding, 'A comparison of performance of six turbulence models', *Proc. NASA Conf. on Free Shear Flows*, Langley, VA, 1972.
2. T. P. Chiang, 'Buoyant jet in flowing stratified field', *Ph.D. Thesis*, Taiwan University, 1988.
3. H. C. Chen and V. C. Patel 'Near-wall turbulence models for complex flow including separation', *AIAA J.*, **26**, 641-648 (1988).
4. W. Rodi, 'Experience with two-layer models combining the $k-\epsilon$ model with a one-equation model near wall', *Proc. 29th Aerospace Science Meet.*, Reno, NV, 1991.
5. W. Rodi, N. N. Mansour and V. Michelassi, 'One-equation near-wall turbulence modeling with the aid of direct simulation data', *J. Fluids Eng.*, **115**, 196-205 (1993).
6. B. Lakshminarayana 'Turbulence modeling of complex shear flows', *AIAA J.*, **24**, 1900-1917 (1986).
7. K. Hanjalic, 'Two dimensional asymmetrical turbulent flow in ducts', *Ph.D. Thesis*, University of London, 1970.
8. B. E. Launder, G. J. Reece and W. Rodi, 'Progress in the development of a Reynolds stress turbulence closure', *J. Fluid Mech.*, **68**, 537-566 (1975).
9. M. Nallasamy, 'Turbulence models and their applications to the prediction of internal flows: a review', *J. Comput. Fluids*, **15**, 151-194 (1987).
10. V. C. Patel, W. Rodi and G. Scheuerer, 'Turbulence models for near-wall and low Reynolds number flows: a review', *AIAA J.*, **23**, 1308-1319 (1984).
11. V. Michelassi and T. H. Shih, 'Low Reynolds number two-equation modelling of turbulent flows', *NASA Technical Memorandum 104368*, 1991.
12. D. M. Driver and H. L. Seegmiller, 'Features of a reattaching turbulent shear layer in divergent channel flow', *AIAA J.*, **23**, 163-171 (1985).
13. J. Rotta, 'Statistical theory of nonhomogeneous turbulence', *Imperial College Report TWF/TN/38, TWF/TN/39*, 1951.
14. J. P. Von-Doormaal and G. D. Raithby, 'Enhancements of the SIMPLE method for predicting incompressible fluid flows', *J. Numer. Heat Transfer*, **7**, 147-163 (1984).
15. D. B. Spalding, 'A novel finite differential expression invoking first and second derivatives', *Int. j. numer. methods eng.*, **4**, 551-559 (1972).

16. R. S. Amano and P. Goel, 'A numerical study of a separating and reattaching flow by using Reynolds-stress turbulence closure', *Numer. Heat Transfer*, **7**, 343–357 (1984).
17. P. G. Huang and M. A. Leschziner, 'Stabilization of recirculating flow computations performed with second-moment closures and third-order discretization', *Proc. 5th Turbulent Shear Flows Conf.*, Ithaca, NY, 1985.
18. A. Brankovic and S. A. Syed 'Validation of Reynolds stress turbulence model in generalized coordinates', *Proc. AIAA 22nd Fluid Dynamics, Plasmadynamics and Lasers Conf.*, Honolulu, HI, 1991, AIAA, New York, 1991.
19. P. S. Klebanoff 'Characteristics of turbulence in boundary layer with zero pressure gradient', *NACA Report 1247*, 1955.
20. E. W. Adams and J. P. Johnston, 'Flow structure in the near-wall zone of a turbulent separated flow', *AIAA J.*, **26**, 932–939 (1988).